

## COUPLING STATIC AND DYNAMIC COMPRESSIONS: FIRST MEASUREMENTS IN DENSE HYDROGEN

P. LOUBEYRE<sup>a,\*</sup>, P. M. CELLIERS<sup>b</sup>, D. G. HICKS<sup>b</sup>, E. HENRY<sup>f</sup>, A. DEWAELE<sup>a</sup>,  
J. PASLEY<sup>c</sup>, J. EGGERT<sup>b</sup>, M. KOENIG<sup>c</sup>, F. OCCELLI<sup>a</sup>, K. M. LEE<sup>d</sup>,  
R. JEANLOZ<sup>d</sup>, D. NEELY<sup>c</sup>, A. BENUZZI-MOUNAIX<sup>c</sup>, D. BRADLEY<sup>c</sup>,  
M. BASTEA<sup>b</sup>, STEVE MOON<sup>b</sup> and G. W. COLLINS<sup>b</sup>

<sup>a</sup>*Département de Physique Théorique et Applications, CEA, Commissariat à l'Energie Atomique, 91680 Bruyères-le-Châtel, France;* <sup>b</sup>*Lawrence Livermore National Laboratory, P.O. Box 808, Livermore, CA 94551, USA;* <sup>c</sup>*LULI Ecole Polytechnique, 91128 Palaiseau, France;*

<sup>d</sup>*Department of Earth and Planetary Science, University of California, Berkeley, CA 94720-4767, USA;* <sup>e</sup>*Central Laser Facility CLRC Rutherford Appleton Laboratory, Chilton, Didcot OX11 0QX, UK;* <sup>f</sup>*Dipartimento di Fisica, Università di Milano-Bicocca, 20126 Milan, Italy*

*(Received 14 August 2003; Revised 27 August 2003; In final form 28 August 2003)*

We demonstrate here a laser-driven shock wave in a hydrogen sample, pre-compressed in a diamond anvil cell. The compression factors of the dynamic and static techniques are multiplied. This approach allows access to a family of Hugoniot curves which span the P–T phase diagram of fluid hydrogen to high density. In this first-of-its-kind experiment, two hydrogen Hugoniot curves have been partially followed starting from pre-compression at pressures of 0.7 GPa and 1.2 GPa. Optical reflectance probing at two wavelengths reveals the onset of the conducting fluid state. The boundary line to conducting fluid hydrogen is suggested.

*Keywords:* Hydrogen; Shock compression; Metallization

An important issue in planetary physics is the accurate determination of the hydrogen equation of state from the molecular fluid to the very dense plasma state [1]. Also, interesting predictions stand out to be tested in dense hydrogen, such as the transition to a metal [2], the existence of a plasma phase transition in the fluid [3], or subtle quantum many body properties of this mixed electrons/protons system [4]. Progress towards understanding hydrogen at high density has recently been achieved by static compression [5], using the diamond anvil cell, and by dynamic compression techniques, using large laser facilities [6], Z-pinch [7] and gas guns [8]. However, the extreme densities relevant to most of the mass of Jupiter (or of any of the extra-solar giant planets) have not been produced in the laboratory and are unreachable by either static or single shock compression techniques alone. In particular, the shock temperature rapidly increases with pressure on the Hugoniot giving a limited compression, which should tend to four-fold for an ideal monatomic gas [9]. One way to achieve higher densities is to use multiple shocks, with stacked laser pulses or with reverberating shock waves [8].

\* Corresponding author. E-mail: paul.loubeyre@cea.fr

But in that case, the thermodynamic state of the system must be calculated from models. The only method to measure the equation of state of very dense hydrogen at planetary core conditions with current technology is to generate the steady propagation of a planar shock front in a pre-compressed sample of hydrogen. The P, V, E state of the system can then be directly measured through the Rankine-Hugoniot equations from shock and particle velocities [9], and temperature can be measured independently with a pyrometric technique. This coupling of static and dynamic compressions seems a simple idea but until now has remained an experimental challenge. The feasibility of a laser-driven planar shock-wave in pre-compressed samples of hydrogen is demonstrated below.

A drawing of the diamond anvil cell (DAC) adapted for laser shock is shown in Figure 1. A strong laser pulse launches a shock in the diamond window. The thickness of the diamond window should be thin enough so that the shock wave could propagate to the sample before side rarefaction waves erode too much the shock planarity. The rarefaction angle in the strained diamond window was measured around  $30^\circ$ . Also, the rarefaction wave launched

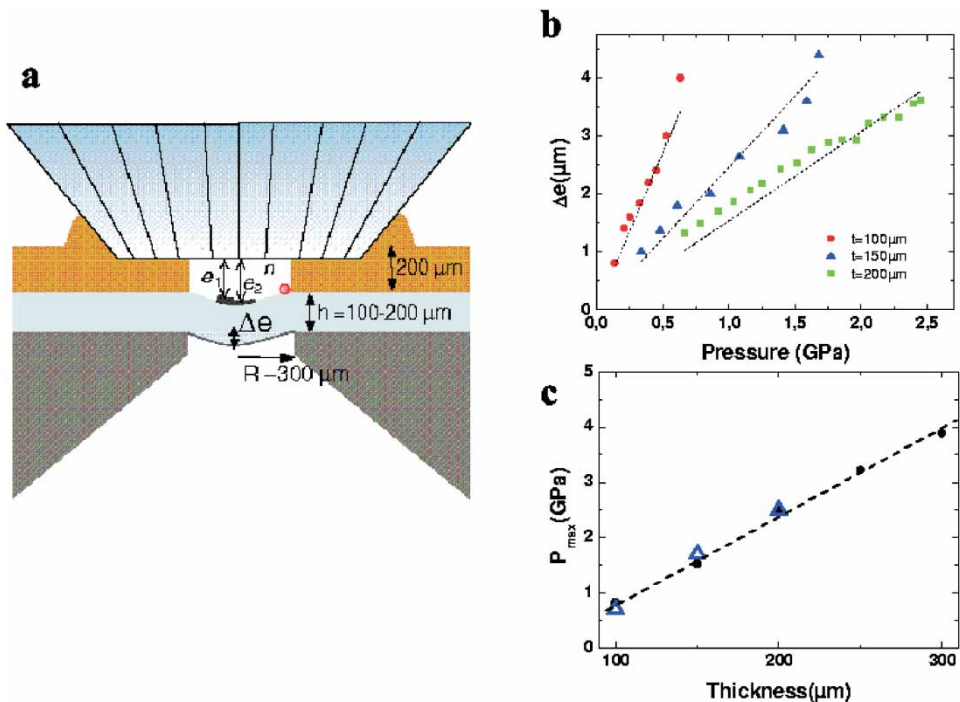


FIGURE 1 Diamond anvil cell configuration used for laser-driven shock on pre-compressed hydrogen and its mechanical behaviour. (a) A diamond anvil with a 1.2 mm tip is pushed against the thin diamond window to apply pressure on the hydrogen sample contained in the centre of a gasket situated in between. The thin diamond window sits on a wide open tungsten-carbide support (here, 600  $\mu\text{m}$  diameter for sufficient optical access to the 400  $\mu\text{m}$  laser spot).  $\Delta e$  indicates the deflection of the diamond window. There is a 100 nm Al flash coating on the rear side of the thin diamond to lower the critical depth of the shock ablation. The diamond anvil has anti-reflection coating for the VISAR measurements. The thickness of the sample chamber is around 100  $\mu\text{m}$  at 1 GPa which allows the propagation of the shock wave in hydrogen for about 5 ns. An Al step and a ruby ball are put on the thin diamond. (b) Deflection of the diamond windows of different thickness versus the pressure in the sample chamber. The symbols are the interferometric measurements and the dashed lines the results of the finite elements calculation, performed using the lowest value of the tensile strength of diamond [21], *i.e.* 3.75 GPa along the [1 1 1] direction, and taking into account the fact that the diamond windows have an [1 0 0] oriented surface. (c) Maximum pressure achieved in the sample chamber versus the thickness of the diamond window. The triangles and dots are respectively the measurements and the finite elements calculation. (This figure can be viewed in colour in the online journal: <http://tandf.co.uk/journals/online/0895-7959.asp>).

at the end of the pulse must not reach the shock front until the wave has propagated through the sample. The pulse characteristics of the laser driver used here has constrained the diamond thickness to be at maximum 200  $\mu\text{m}$ . The mechanical behaviour of the diamond disc was obtained by a finite element calculation that takes into account the elastic strain of the thin diamond support. As seen in Figure 1, this calculation can reliably predict the deflection of the diamond disk measured experimentally by a combination of white light and monochromatic interferences [10] and the maximum pressure that can be achieved for a given diamond thickness. With a thickness of 200  $\mu\text{m}$  over an aperture of 600  $\mu\text{m}$  diameter, a pre-compressed hydrogen sample at 2.5 GPa can be obtained. Determining the pressure-density-internal energy conditions in the pre-compressed sample,  $P_0$ ,  $\rho_0$ ,  $E_0$ , is essential for Hugoniot measurements.  $P_0$  is measured with the ruby fluorescence pressure gauge [11].  $\rho_0$  and  $E_0$  are estimated by an accurate EOS of fluid hydrogen [12]. Two successful laser shocks in pre-compressed samples of hydrogen demonstrate the feasibility and reproducibility of the technique. Hydrogen was pressurized at 300 K respectively to 0.7 GPa ( $\rho_0 = 0.061 \text{ mol/cm}^3$ ) and to 1.2 GPa ( $\rho_0 = 0.073 \text{ mol/cm}^3$ ) which represents a significant increase of the initial density compared to the cryogenic targets ( $0.042 \text{ mol/cm}^3$ ). The refractive index of the pre-compressed hydrogen sample and the thickness of hydrogen in between the Al step and the surface of the diamond anvil, *i.e.* the transit gap for the shock wave propagation in hydrogen, were accurately determined by interferometric measurements [10]. The shock was driven by a laser pulse ( $10^{14} \text{ W/cm}^2$  for 1.2 ns; with a 400  $\mu\text{m}$  spot in diameter spatially smoothed; by way of seven beams, six of which come from off axis at  $16^\circ$ ). The shock amplitude was high enough to make the shock front reflecting the 1064 nm probe laser beam of the velocity interferometric system for any reflector (VISAR). This diagnostic is used to characterize the kinematic parameters of the shock and the optical properties of compressed hydrogen [13]. Figure 2 shows the fringe pattern produced by the velocity interferometer for the DAC initially at 0.7 GPa. The phase shift has been converted into velocity along several lineout windows on each sides of the Al step. As seen in Figure 2, the trajectories derived from these velocity curves reproduce the transit gap and the Al step height deduced from the interferometric determination in the sample before the shock. This verifies that the 1064 nm VISAR is probing the moving reflecting front of a planar shock wave in hydrogen. The shock pressure and density were determined from shock and particle velocities,  $U_s$  and  $U_p$ , and the Rankine-Hugoniot relations [9]. The particle velocity,  $U_p$ , is estimated by standard impedance matching with aluminium knowing the shock speed in Al, as measured from the transit time in the Al step by the VISAR [7]. Our  $P$ ,  $\rho$  data in both DACs agree with the standard SESAME equation of state [14] but the error bars are large, essentially because of the large uncertainties in the shock speeds (8% for the shock speed in Al and 2% for the shock speed in hydrogen). It should be noted that the access to lasers of few KJoule energy will enable the shock to be driven over a longer time and on a larger diameter. Then,  $P$ ,  $\rho$  data should be obtained with a similar accuracy as in cryo-targets [7]. Also, thicker diamond windows could be used to pre-compress the sample to higher pressure.

On the other hand, reflectivity data can be determined confidently with a decaying shock since the VISAR diagnostic provides a simultaneous measurement of velocity and reflectance of the shock front. As can be seen in Figure 2, the reflectance drops at shock breakout from Al into hydrogen, and then continuously decays with the shock velocity through the transit gap. The shock front can be considered as a specular reflector and therefore the reflectivity of the shock front is amenable to Fresnel analysis, that is directly related to the complex refractive index of compressed hydrogen [15]. The reflectance in hydrogen was calibrated relative to the measured reflectance on the Al step, leading to a jump from 90% to around 20% reflectance at shock breakout. The shock velocity measured at the hydrogen shock front was converted to

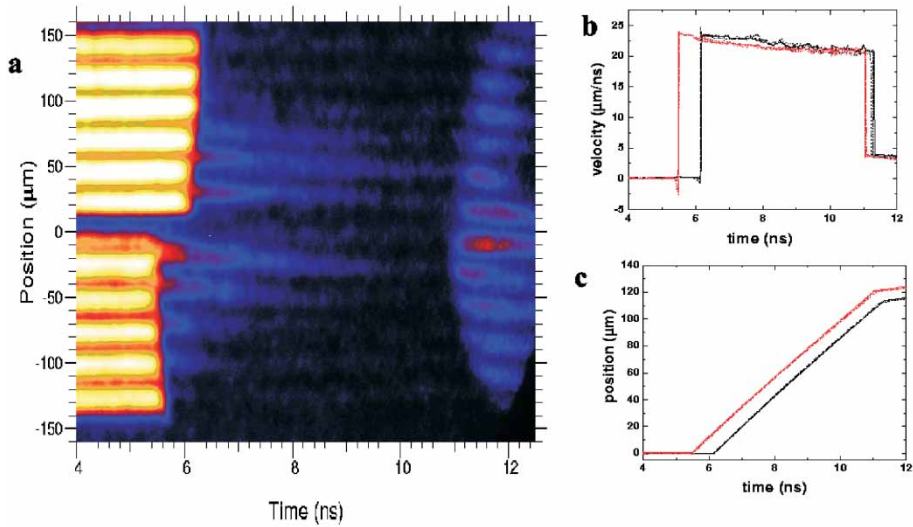


FIGURE 2 (a) Light at 1064 nm wavelength reflected from the shock front in hydrogen precompressed to 0.7 GPa observed through the velocity interferometer and the shock velocity versus time. Before 5.4 ns the stationary fringes are produced by the reflection of the probe beam from the stationary Al step/hydrogen interface. At  $\sim 5.5$  ns (6.2 ns) the shock breaks out from the thin (thick) aluminium step, launching a strong shock wave in hydrogen. The fringes shifted continuously down (deceleration) as the shock decayed. At  $\sim 11$  ns, the shock in the pre-compressed hydrogen collides with the diamond anvil on the rear of the cell. This event is easily identified by the sudden increase in the reflectance. (b) Velocity versus time. (c) Trajectories versus time (produced by integrating the velocity data in time to get the shock position). The grey and black curves correspond each to 3 lineout windows on a distance of 50  $\mu\text{m}$ , plotted as dashed, dotted and full curves (hardly visible), respectively in front of the thin and thick Al steps. The dispersion of the velocity of the various lineout windows over a distance of 50  $\mu\text{m}$  is less than  $\pm 2\%$ . (This figure can be viewed in colour in the online journal: <http://tandf.co.uk/journals/online/0895-7959.asp>).

pressure, density and temperature of the compressed hydrogen by using the SESAME equation of state [14]. The continuous record of reflectance versus shock velocity obtained with the VISAR (1064 nm) is thus plotted as reflectance versus pressure and reflectance versus temperature along the two Hugoniot curves in Figure 3. Another VISAR diagnostic, VISAR (532 nm), was operated in both shots with a laser probe at 532 nm. The VISAR (532 nm) data are not compatible with the VISAR (1064 nm) data under the assumption that the Doppler shift is produced by reflection from the shock front. Also, the reflectivity was observed to be decaying faster and to be greater at 532 nm than at 1064 nm. Consistency between the two VISARs is recovered under the assumptions that the 532 nm light is reflected at the aluminium pusher–hydrogen interface. The Al/hydrogen interface velocity then obtained is close to that measured for the pusher velocity. Consequently, the decaying reflectivity is related in this case to the extinction depth at 532 nm in compressed hydrogen, which is estimated to be of the order of  $10 \pm 5 \mu\text{m}$  in the density–pressure–temperature range covered here.

A 10% optical reflectance is evidence that shocked hydrogen is becoming a conductive fluid. In a previous laser shock study on cryogenic deuterium [15], shock reflectance at 1064 nm was seen to increase continuously along the Hugoniot beginning at about 20 GPa up to a limit value above 50 GPa. This evolution was analysed as the gradual transformation of hydrogen to a conducting fluid. The saturation value was interpreted as full ionisation of hydrogen within a framework of the Drude model under the assumption of the Ioffe-Regel formulation for the relaxation time of the electrons. With the same Drude model, the observation of a reflectance about 10% at 1064 nm gives an ionisation fraction of about 1%.

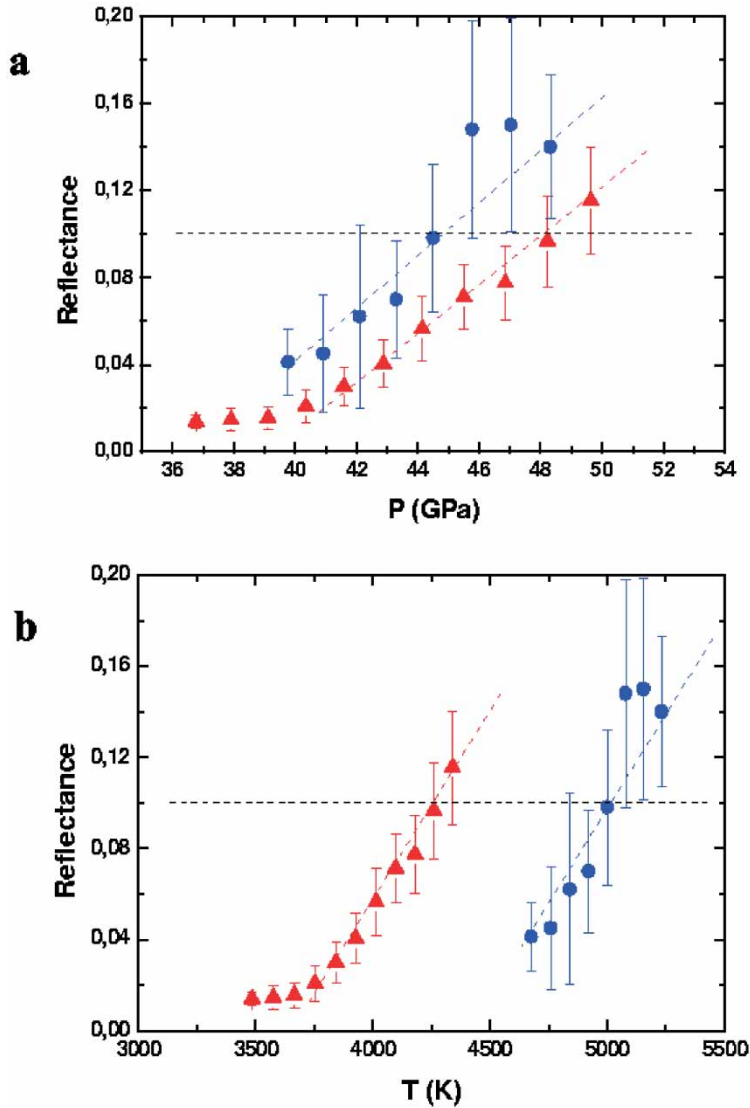


FIGURE 3 Shock front reflectance as a function of pressure (a) and temperature (b). The  $P$ - $T$  conditions are calculated from the measured shock velocity with the SESAME equation of state [14]. The dots and triangles indicate respectively the data points along the Hugoniot curves of hydrogen initially pre-compressed to 0.7 and 1.2 GPa. (This figure can be viewed in colour in the online journal: <http://tandf.co.uk/journals/online/0895-7959.asp>).

The absorption depth of  $10\ \mu\text{m}$  at  $532\ \text{nm}$  essentially constrains the value of relaxation time to 20 times the one of the Ioffe-Regel formulation. This is a surprisingly large value but the Drude model may not be valid in this region of small ionisation concentration. Indeed, a breakdown of the Drude model at low carrier concentrations has been recently demonstrated in a first-principles molecular dynamic simulation with the frequency-dependent conductivity computed with the Kubo-Greenwood formula for fluid hydrogen [16].

Various calculations [16–19] agree on the same microscopic description of fluid hydrogen at high pressure, *i.e.* there is a close relationship between conductivity and dissociation. An ionisation fraction of about 1% should correspond to a dissociation fraction in the range of

5–10%. The 1% ionisation fraction seems a good criterion to set the boundary between insulating and conducting fluid hydrogen because then the transport, optical and thermodynamic properties of the fluid should be appreciably affected by ionisation. This criterion is used, in Figure 4, to plot, as circles, the data points of the transition to the conducting state as extracted from the reflectance measurements along the Hugoniot generated by laser shock on cryo-deuterium [15] and on the two precompressed targets of the present study. The error bars mainly arise from the uncertainty in the reflectance data. The gas gun [8] reverberating shock experiment has also probed the transition to the conductive state but in different pressure–temperature ranges. Two limiting models can be used to correlate the detection to the conductive state either from the reflectivity or from conductivity measurements. First, following first principle molecular dynamic simulation [16], a reflectivity of about 10% should correspond to a conductivity of few  $(\Omega\text{cm})^{-1}$ . Second, following the Drude model with the Ioffe-Regel relaxation time, an ionisation fraction of 1% at the density of the gas gun experiment gives a conductivity of about  $300 (\Omega\text{cm})^{-1}$ . The triangle in Figure 4 indicates the transition to the conductive state inferred from the gas gun conductivity data, and the error bars come from the uncertainty of the model based correlation. The lighter dashed-line in Figure 4 shows the transition between fluid molecular hydrogen and conductive fluid hydrogen.

Two important messages that we want to convey here are illustrated in Figure 4. First, laser shocks on pre-compressed samples of hydrogen offer a unique opportunity to cover the P–T domain of fluid hydrogen or other compressible samples like He, H<sub>2</sub>O or H<sub>2</sub>/He mixtures. In the case of the important astrophysical H<sub>2</sub>/He mixture, pressurization is the only way to produce a uniform single phase target sample. The domain accessible in a near future, indicated as grey, is the envelope of Hugoniot curves bounded by the principal Hugoniot of the cryogenic liquid state and the Hugoniot of the room-temperature initial state at 5 GPa. This domain should be significantly extended with the access to the next generation of few KJ lasers. With the same technique and the same diagnostics we will be able to accurately probe the boundary lines for dissociation, ionisation, conductivity or miscibility and measure the equation of state. Second, planetary isentropes reach much higher densities that can be

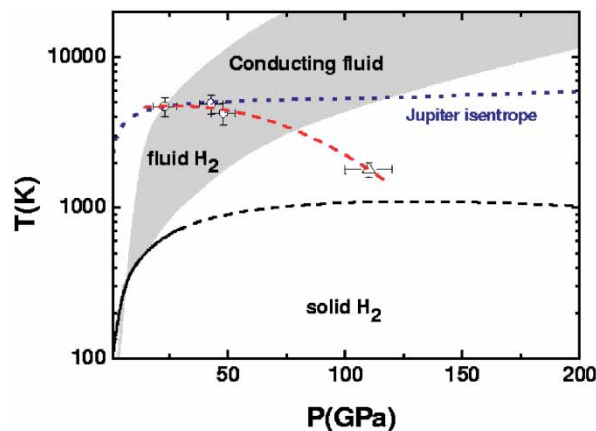


FIGURE 4 Phase diagram of fluid hydrogen. The solid line represents the determination of the melting curve of hydrogen [20] and its extrapolation (dashed). The grey area is the envelope of the Hugoniot curves in between the Hugoniot of cryo-hydrogen and the Hugoniot of hydrogen initially at 5 Gpa. The dashed upper line is the isentrope of Jupiter [22]. The dashed line between indicates the transition to conducting fluid hydrogen. The symbols are extracted from experiment as explained in the text: dots, from laser shock (Ref. [15] and present study) and triangle from gas gun study [8]. (This figure can be viewed in colour in the online journal: <http://tandf.co.uk/journals/online/0895-7959.asp>).

achieved with standard shock compression. By using pre-compressed targets, we will be able to recreate a large fraction of the planetary core conditions of Jupiter and consequently provide a direct observational constraint on planetary and stellar structure models.

### *Acknowledgements*

The laser shocks were performed with the Vulcan laser at the Rutherford Appleton Laboratory.

### *References*

- [1] D. J. Stevenson and F. E. Salpeter, *The Astrophys. Journal Supplement Series*, **35**, 221 (1977).
- [2] E. E. Wigner and H. B. Huntington, *J. Chem. Phys.*, **3**, 764 (1935).
- [3] D. Saumon and D. G. Chabrier, *Phys. Rev. Lett.*, **62**, 2397 (1989).
- [4] E. G. Maksimov and Y. I. Shilov, *Physics-Uspokhi*, **42**, 1121 (1999).
- [5] P. Loubeyre, F. Occelli and R. LeToullec, *Nature*, **416**, 613 (2002).
- [6] G. W. Collins *et al.*, *Science*, **281**, 1178 (1998).
- [7] M. D. Knudson *et al.*, *Phys. Rev. Lett.*, **87**, 225501 (2001).
- [8] S. T. Weir, A. C. Mitchell and W. J. Nellis, *Phys. Rev. Lett.*, **76**, 1860 (1996).
- [9] Y. B. Zeldovich and Y. B. Raizer, *Physics of Shock Waves and High Temperature Phenomena* (Academic Press, New York 1967).
- [10] A. Dewaele, J. Eggert, P. Loubeyre and R. LeToullec, *Phys. Rev. B*, **67**, 094112 (2003).
- [11] H. K. Mao, J. Xu and P. M. Bell, *J. Geophys. Res. B*, **91**, 4673 (1986).
- [12] R. L. Mills, D. H. Liebenberg, J. C. Bronson and L. C. Schmidt, *J. Chem. Phys.*, **66**, 3076 (1977).
- [13] P. M. Celliers *et al.*, *Appl. Phys. Lett.*, **73**, 1320 (1998).
- [14] G. I. Kerley, In: J. M. Haile and G. A. Mansoori (Eds.) *Molecular-Based Study of Fluids* (American Chemical Society, 1983), pp. 107–138.
- [15] P. M. Celliers *et al.*, *Phys. Rev. Lett.*, **84**, 5564 (2000).
- [16] L. A. Collins *et al.*, *Phys. Rev. B*, **63**, 184110 (2001).
- [17] T. Lenosky, J. Kress, L. Collins and I. Kwon, *Phys. Rev. B*, **55**, 11907 (1997).
- [18] R. Redmer, G. Ropke, S. Kuhlbrodt and H. Reinholz, *Phys. Rev. B*, **63**, 233104 (2001).
- [19] O. Pfaffenzeller and D. Hohl, *J. Phys.: Condens. Matter*, **9**, 11023 (1997).
- [20] F. Datchi, P. Loubeyre and R. LeToullec, *Phys. Rev. B*, **61**, 6535 (2000).
- [21] J. E. Field, *The Properties of Diamond* (Academic Press, London 1992), p. 484.
- [22] T. Guillot, *Planet. Space Sci.*, **47**, 1183–1200 (1999).